Semiconductor Physics, Quantum Electronics & Optoelectronics, 2026. V. 29, No 3. P. 354-360.

Semiconductor physics

Spectroscopic ellipsometry evidence of Mn level hybridization in (Ga,Mn)(As,P)

O.B. Yastrubchak[1,*], S.V. Mamykin[1], V.R. Romanyuk[1], O.S. Kondratenko[1], L.V. Borkovska[1], L.Yu. Khomenkova [1], V.V. Kalyuzhny[1], O.V. Shtykalo[1], O.F. Kolomys[1], X. Liu[2], J.K. Furdyna[2], B.A. Assaf[2]

[1]*V. Lashkaryov Institute of Semiconductor Physics, NAS of Ukraine, 03028 Kyiv, Ukraine*
[2]*Department of Physics and Astronomy, University of Notre Dame, Notre Dame, IN 46556, USA*
[*]*Corresponding author e-mail: plazmonoki@gmail.com*

Abstract. We demonstrate direct spectroscopic control of Mn-derived electronic states in the diluted ferromagnetic semiconductor (Ga,Mn)(As,P) *via* phosphorus incorporation at fixed Mn concentration. Using spectroscopic ellipsometry, we observe a systematic evolution from strongly *p–d* hybridized Mn–valence-band states at low P content to localized, atomic-like Mn *d*-derived states at high P content. This evolution is manifested by a transition from broad optical absorption features (2.0–2.8 eV), which weaken upon annealing, to a sharp, annealing-insensitive absorption peak (2.6–2.9 eV), accompanied by a P-dependent shift of the valence band relative to the Fermi level. These results establish phosphorus substitution as an independent control parameter for Mn–host matrix electronic hybridization, decoupled from Mn concentration. The systematic evolution of the Mn-related spectral features indicates that P incorporation can modify the balance between more delocalized, valence-band–like and more localized Mn-derived states. Our spectroscopic results indicate that the nature of Mn-related states depends on the material composition.

Keywords: dilute ferromagnetic semiconductors, *p–d* hybridization, (Ga,Mn)(As,P) alloys, spectroscopic ellipsometry.

https://doi.org/10.15407/spqeo29.03.354
PACS 71.20.Nr, 75.50.Pp, 78.20.Ci, 78.40.Fy

Manuscript received 19.08.26; revised version received 07.09.26; accepted for publication 16.09.26; published online 25.09.26.

1. Introduction

Ferromagnetic semiconductors (FMSs) based on III–Mn–V alloys are prototypical systems for exploring the interplay between spin and charge degrees of freedom and have played an important role in the development of semiconductor spintronics [1–3]. In these materials, Mn simultaneously provides localized magnetic moments and hole carriers, enabling carrier-mediated ferromagnetic coupling [4–6]. Consequently, the magnetic and electronic properties are intrinsically intertwined, with the Mn concentration and carrier density influencing both the exchange interaction and the electronic structure [1–6]. This intrinsic coupling makes independent control of magnetic exchange and the electronic band structure challenging.

A key route to overcome this limitation is chemical alloying of the host lattice (for example with Bi ions), which modifies band structure and impurity levels without directly altering Mn content [7–10].

(Ga,Mn)(As,P) offers a unique platform in which the electronic structure can be tuned *via* the As/P ratio, in addition to Mn concentration and thermal processing as well [11]. In this system, substitutional Mn on Ga sites acts as an acceptor whose binding energy increases significantly from ~ 0.11 eV in (Ga,Mn)As [12] to ~ 0.4 eV in (Ga,Mn)P [13], suggesting a continuous tuning of the degree of *p–d* hybridization with increasing P content.

Despite extensive studies, the fundamental nature of Mn-derived electronic states in III–Mn–V ferromagnetic semiconductors remains unresolved: whether they form valence-band–hybridized states or more localized impurity-like states. This distinction is governed by the strength of hybridization between Mn 3*d* states and anion *p* states, which ultimately controls the character of the exchange interaction.

Here, we employ spectroscopic ellipsometry (SE) to probe the evolution of Mn-derived electronic states in (Ga,Mn)(As,P) as a function of phosphorus concentration and post-growth annealing.

2. Materials and methods

We studied 30-nm-thick $(Ga_{1-x}Mn_x)(As_{1-y}P_y)$ layers with a fixed Mn concentration x = 0.07 and phosphorus concentration (y) varying within 0.11–0.31. All samples were grown using molecular beam epitaxy (MBE) at 230 °C on (001)-oriented p-type GaAs substrates. After growth, the (Ga,Mn)(As,P) layers were annealed at 250 °C for 1 h under nitrogen flow to improve their magnetic and transport properties by promoting out-diffusion of Mn interstitials.

The quality of the samples used in this study is confirmed by high-resolution X-ray diffraction (HRXRD). 2θ-ω coupled diffraction scans along the growth direction (which, for convenience, we will refer to as the c-direction) were performed on each thin film specimen using a Bruker D8 Discover high-resolution X-ray diffractometer. The mole fractions of Mn and P in the thin films can be accurately calculated based on this XRD analysis, considering that $Ga(As_{1-y}P_y)$ and $(Ga_{1-x}Mn_x)(As_{1-y}P_y)$ films are coherently strained by the GaAs buffer layer.

Magnetic properties of both as-grown and annealed (Ga,Mn)(As,P) films in the sample series were investigated using a Quantum Design MPMS XL SQUID magnetometer. Temperature-dependent measurements were performed with the magnetic field applied perpendicular to the film plane (along the [001] axis) with a strength of 20 Oe. Corresponding hysteresis loops were measured at T = 5 K. The Curie temperature (T_C) and low-field saturation magnetization at 5 K were estimated from SQUID magnetometry data.

The optical dielectric function of each layer is then measured using spectroscopic ellipsometry (SE) [14, 15]. SE probes the near-surface region, depending on the penetration depth of the applied polarized light. The SE experiments have been conducted at room temperature using the SE-2000 Semilab multi-angle spectroscopic ellipsometer (working wavelength range: 250 to 2100 nm) capable of determining the optical properties of the layers and their thicknesses. The spectral dependences of the ellipsometry angles, Ψ(λ) and Δ(λ), are obtained from the SE measurements and used to calculate the effective complex dielectric function, $\varepsilon_1 + i\varepsilon_2$, of the layered material under investigation. Here, ε_1 and ε_2 represent the real and imaginary parts of the dielectric function, respectively.

Table 1. Sample list with the lattice parameters and the out-of-plane strain $\varepsilon_\perp$.

$(Ga_{1-x}Mn_x)(As_{1-y}P_y)$	Lattice parameters (Å)		Out-of-plane strain $\varepsilon_\perp$ (%)
	Vertical, c	Relaxed, a_{relax}	
$x = 0, y = 0.05$	5.6332	5.6427	–0.168
$x = 0, y = 0.15$	5.5959	5.6230	–0.482
$x = 0.07, y = 0.11$	5.64330	5.6480	–0.083
$x = 0.07, y = 0.26$	5.5885	5.6191	–0.545
$x = 0.07, y = 0.31$	5.5675	5.6080	–0.722

3. Experimental results

3.1. High-resolution X-ray diffraction

All epitaxial layers exhibited excellent crystalline quality [11, 12] and were grown under tensile strain, as shown in Fig. 1.

This strain is characterized by the misfit f and the out-of-plane strain $\varepsilon_\perp$. The component of the strain tensor perpendicular to the film/substrate surface is defined as:

$$\varepsilon_\perp = (c - a_{relax})/a_{relax}, \quad (1)$$

where c is the vertical lattice parameter, and a_{relax} is the relaxed lattice parameter, calculated from HRXRD data. The strain value is smaller for all (Ga,Mn)(As,P) layers compared to Ga(As,P) layers with a similar As:P ratio and is consistent with Mn partially compensating the lattice mismatch generated by the introduction of P.

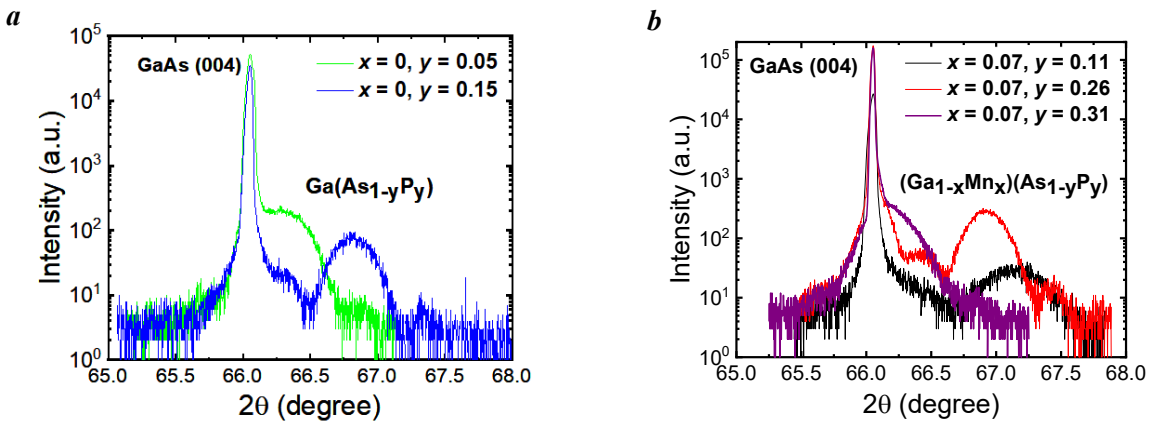

Fig. 1. HR-XRD spectra for 2θ-ω coupled scans on the series of pristine (*a*) $Ga(As_{1-y}P_y)$ and (*b*) $(Ga_{1-x}Mn_x)(As_{1-y}P_y)$ epitaxial layers grown on p-type (001) GaAs substrates. The concentrations of Mn and P for each sample shown in the figure were calculated based on these spectra.

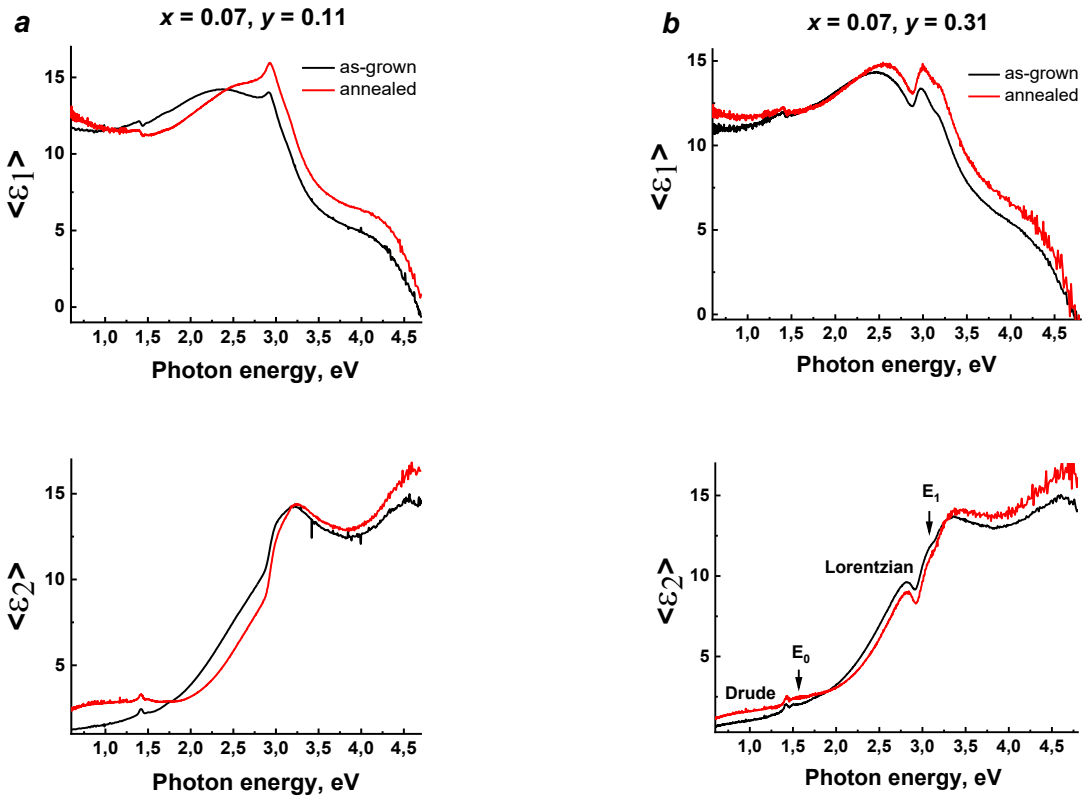

Fig. 2. Spectral dependences of the real part ε_1 and imaginary part ε_2 of the pseudo-dielectric function for as-grown and annealed $(Ga_{0.93}Mn_{0.07})(As_{0.89}P_{0.11})$/GaAs (*a*), $(Ga_{0.93}Mn_{0.07})(As_{0.69}P_{0.31})$/GaAs (*b*) heterostructures. The arrows indicate the energy positions of E_0 and E_1.

3.2. Spectroscopic ellipsometry results

We discuss the spectroscopic ellipsometry measurements within 0.5 to 5 eV. Fig. 2 shows the experimental real (top row) and imaginary (bottom row) parts of the dielectric function for all as-grown and annealed (Ga,Mn)(As,P) layers, as well as for the Ga(As,P) reference samples. Several features become evident upon comparison between the reference and Mn-containing samples. (i) The overall spectral shape is similar across all samples, showing an increase in absorption up to nearly 3 eV, followed by a minimum in ε_2 between 3.5 and 4.0 eV. (ii) For y = 0.11 (Fig. 2a), a pronounced low-energy spectral weight emerges below 1.5 eV, particularly after annealing, which is attributed to free-carrier absorption. (iii) As shown in Fig. 2b, increasing *y* progressively suppresses the free-carrier contribution.

However, a significant amount of spectral weight builds up at higher energies, which, for $y = 0.31$, can be resolved as an additional absorption feature, modeled by a Lorentzian term in Fig. 2b. The quantitative analysis presented below provides insight into the origin of these features and the evolution of the electronic structure with increasing P concentration.

We employ a model based on a set of critical-point energies and the corresponding formalism developed by Adachi to describe the dielectric function of all films. These critical-point energies include the optical band gap E_0 and E_1, which correspond to the $L_{4,5} \rightarrow L_6$ optical transition commonly observed in III–V semiconductors. The modeling and fitting procedure were performed using Semilab SEA (Win Elli 3) software (v1.7.9).

To investigate the optical properties of GaAs-based materials, we employed a model based on the set of critical-point energies. These energies include E_0, $E_0 + \Delta_0$ (with a valence band split-off energy Δ_0), E_1, $E_1 + \Delta_1$, E_2, $E_2 + \Delta_2$, and E_0'. Furthermore, we accounted for the contribution of free electrons to light scattering, described by the Drude component of the complex dielectric function. This allowed us to estimate the concentration level (N) and mobility (μ) of free holes. The dielectric function $\varepsilon_D(E)$ related to the Drude component for ellipsometric data analysis can be expressed by the following equation:

$$\varepsilon_D(E) = \varepsilon_1(E) + i\varepsilon_2(E), \qquad (2)$$

where the real part of the dielectric permittivity is $\varepsilon_1(E) = -\dfrac{(E_p/E)^2}{1+(E_\Gamma/E)^2}$, and the imaginary part of the dielectric permittivity is $\varepsilon_2(E) = \dfrac{E_\Gamma}{E}\dfrac{(E_p/E)^2}{1+(E_\Gamma/E)^2}$. The parameters E_p and E_Γ represent the plasma energy and the broadening, respectively, which is associated with the scattering frequency.

Table 2. Sample list showing the optical band gap E_0, Lorentzian-shaped transition E_L, free hole concentration N, and Curie temperature T_C.

$(Ga_{1-x}Mn_x)(As_{1-y}P_y)$	E_0 (eV)	E_L (eV)	N (cm^{-3})	T_C (K)
$x = 0$, $y = 0.05$	1.458	–	–	–
$x = 0$, $y = 0.15$	1.534	–	–	–
$x = 0.07$, $y = 0.11$	1.500	2.675	6.55E + 20	60
$x = 0.07$, $y = 0.11$ annealed	1.490	2.723	1.61E + 21	110
$x = 0.07$, $y = 0.26$	1.485	2.684	7.18E + 20	30
$x = 0.07$, $y = 0.26$ annealed	1.472	2.600	6.03E + 20	70
$x = 0.07$, $y = 0.31$	1.466	2.888	1.44E + 20	27
$x = 0.07$, $y = 0.31$ annealed	1.495	2.830	3.20E + 20	70

The results of the SE measurements and the corresponding fits are presented in Table 2 and depicted in Fig. 2. The evolution of the main optical transitions E_0 and E_L for the epitaxial layers are presented in Fig. 3. The experimental data for Ga(As,P) are compared with the calculated dependence shown in Fig. 3 as black dashed lines, which account for the tensile strain estimated from HRXRD measurements.

In Fig. 3a, we plot E_0 with respect to the out-of-plane strain determined from X-ray diffraction. For the (Ga,Mn)(As,P) layers, E_0 is consistently lower in energy compared to Ga(As,P) and does not exceed 1.495 eV. The nearly constant E_0 is consistent with a picture of the band structure where the Fermi level remains pinned, as the valence band edge drops in energy with increasing P. Again, for Ga(As,P), E_0 increases with increasing $|\varepsilon_\perp|$, but for (Ga,Mn)(As,P), it remains unchanged.

The electronic band structure of $Ga(As_{1-y}P_y)$ epitaxial layers grown on (001) GaAs substrates was analyzed to determine the effect of composition and epitaxial strain on the optical band gap. The unstrained (bulk) band gap at 300 K was calculated using the standard empirical relation:

$$E_0(y) = 1.424 + 1.150y + 0.176y^2 . \quad (3)$$

The out-of-plane ($\varepsilon_\perp$) strain components were evaluated. The measured vertical lattice parameter (c) is smaller than the relaxed lattice parameter (a_{relax}) for both samples, confirming an in-plane biaxial tension with corresponding out-of-plane compressive deformation.

Biaxial tensile strain modifies the band structure through two primary mechanisms: a hydrostatic deformation, which shrinks the overall band gap, and a shear deformation, which lifts the degeneracy of the valence band at the Γ-point. Under biaxial tension, the light hole (LH) band shifts above the heavy hole (HH) band, determining the new fundamental band edge.

4. Discussion

The SE results provide a coherent picture of how phosphorus incorporation modifies the character of Mn levels in (Ga,Mn)(As,P). The nature of the Mn-induced acceptor state evolves as a function of its energetic separation from the valence-band maximum [18]. When the acceptor level lies close to the valence-band edge, the Mn states retain a predominantly *p-d* hybridized, valence-band–like character and remain partially delocalized over neighboring anion sites. As the valence-band

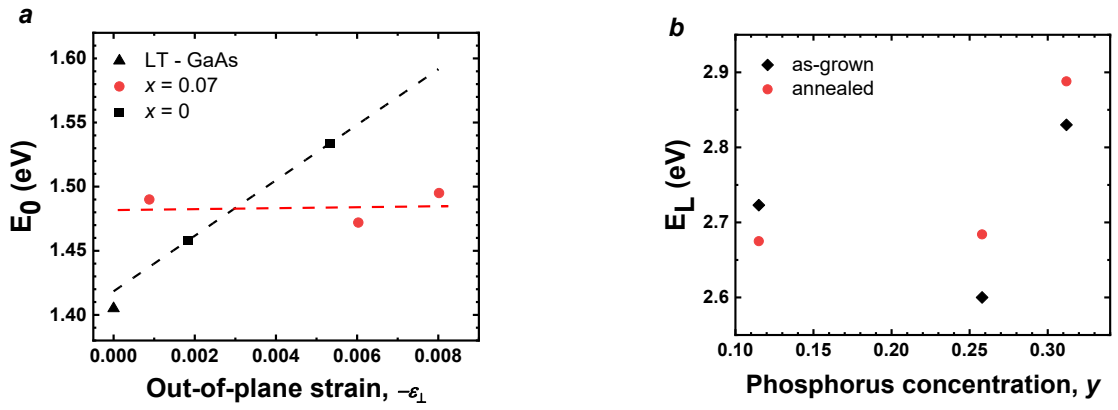

Fig. 3. E_0 as a function of out-of-plane strain, $\varepsilon_\perp$ (*a*) for Ga(As,P) and annealed (Ga,Mn)(As,P). (*b*) E_L *versus* P concentration for as-grown and annealed (Ga,Mn)(As,P). The black dashed lines plot the behavior of E_0 calculated for Ga(As,P) considering the impact of strain, with values taken from Table 1. The red dashed line is a guide to the eye.

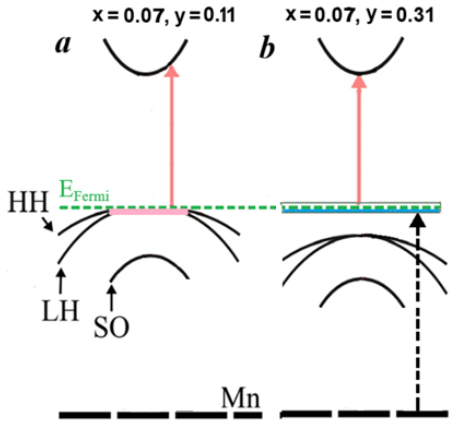

Fig. 4. Schematic energy band diagrams for the (*a*) $(Ga_{0.93}Mn_{0.07})(As_{0.89}P_{0.11})$, (*b*) $(Ga_{0.93}Mn_{0.07})(As_{0.69}P_{0.31})$ layers in the vicinity of the Γ point of the Brillouin zone, illustrating the emergence of a separated Mn-derived impurity band with increasing P content. The solid red arrows indicate the optical E_0 transition. The Fermi level is shown by the green dashed line. HH, LH, and SO parabolas denote the heavy-hole, light-hole, and spin-orbit split-off bands, respectively. The thick dashed black line denotes the Mn *d* core level, while the black dashed arrow indicates transitions from this core level to the Mn impurity levels in the gap. The *p*–*d* hybridized states near the valence-band edge are shown in pink in (*a*), whereas the Mn *d*-derived states forming the separated impurity band are shown in blue in (*b*).

edge shifts further away from the Mn levels with increasing the P concentration, the Mn states acquire a progressively more Mn-centered character. This results in stronger localization of the Mn 3*d* orbitals and may eventually lead to the formation of a separated impurity band. [19]. These strongly localized states give rise to pronounced atomic-like *d*–*d* transitions, which are clearly resolved as a distinct E_L maximum in the SE spectra. The spectral position and the intensity of the feature associated with the Mn-derived states depend on the P content and annealing.

Our main finding is summarized in Fig. 4, where we illustrate the possible tuning of Mn impurity-state hybridization by P doping. The hybridization of Mn states in III–V compounds has previously been investigated by first-principles calculations by P. Mahadevan and A. Zunger [20]. Their model shows that, in GaAs, Mn states are strongly hybridized with valence-band states, forming so-called dangling-bond hybrid (DBH) states. In contrast, in GaN, the Mn states are predominantly localized on the transition-metal ion and are described as crystal-field resonances (CFRs). In (Ga,Mn)(As,P), we observe a similar crossover from a DBH-like state at low P concentrations to a CFR-like state at high P concentrations.

Our SE measurements additionally reveal Fermi-level pinning, which renders the E_0 transition energy nearly independent of P concentration. Nevertheless, our results demonstrate that (Ga,Mn)(As,P) provides a versatile platform for systematically tuning the fundamental properties of impurity states through chemical composition.

Acknowledgement

The financial support (Project number 2025.07/0271 "Band Structure Engineering in Mn- and Fe-Doped Multicomponent Dilute-Ferromagnetic Semiconductors and Topological Semimetals for Photonic and Spintronic Device Applications") from the National Research Foundation of Ukraine for this research is gratefully acknowledged.

References

1. Bonanni A., Dietl T., Ohno H. Dilute magnetic materials**.** In: *Handbook of Magnetism and Magnetic Materials*, M. Coey and S. Parkin (Eds.). Springer, Cham, 2021. P. 923–978. https://doi.org/10.1007/978-3-030-63210-6_21.
2. Takeda Y., Ohya S., Hai P. *et al.* Direct observation of the magnetic ordering process in the ferromagnetic semiconductor $Ga_{1-x}Mn_xAs$ *via* soft X-ray magnetic circular dichroism. *J. Appl. Phys.* 2020. **128**. P. 213902. https://doi.org/10.1007/10.1063/5.0031605.
3. Need R.F., Bac S.-K., Liu X. *et al*. Magnetic properties and electronic origin of the interface between dilute magnetic semiconductors with orthogonal magnetic anisotropy. *Phys. Rev. Mater.* 2020. **4**. P. 054410. https://doi.org/10.1007/10.1103/PhysRevMaterials.4.054410.
4. Yuan Y., Xie Y., Yuan N. *et al.* The Al doping effect on epitaxial (In,Mn)As dilute magnetic semiconductors prepared by ion implantation and pulsed laser melting. *Materials*. 2021. **14**. P. 4138. https://doi.org/10.3390/ma14154138**.**
5. Kalita H., Bhushan M., Singh L.R. A comprehensive review on theoretical concepts, types and applications of magnetic semiconductors. *Mater. Sci. Eng. B*. 2023. **288**. P. 116201. https://doi.org/10.1016/j.mseb.2022.116201**.**
6. Jira E.T., Berry H.D. The study of transport properties of (III−Mn)V diluted magnetic semiconductors. *Adv. Condens. Matter Phys.* 2023. **2023**. P. 8860586. https://doi.org/10.1155/2023/8860586.
7. Tataryn N., Gluba L., Yastrubchak O. *et al*. Valence band dispersion in Bi-doped (Ga,Mn)As epitaxial layers. *IEEE Trans. Magn*. 2023. **59**. P. 4100405. https://doi.org/10.1109/TMAG.2023.3284538.
8. Yastrubchak O., Tataryn N., Gluba L. *et al*. Influence of Bi doping on the electronic structure of (Ga,Mn)As epitaxial layers. *Sci. Rep*. 2023. **13**. P. 17278. https://doi.org/10.1038/s41598-023-43702-w.
9. Wosinski T. Bismuth doping-induced enhancement of the spin–orbit coupling strength in the prototype dilute ferromagnetic semiconductor (Ga, Mn)As: A review. *J. Electron. Mater.* 2025. **54**, No 6. P. 4275–4286. https://doi.org/10.1007/s11664-025-11923-6.
10. Andrearczyk T., Levchenko K., Sadowski J. *et al*. Structural quality and magnetotransport properties of epitaxial layers of the (Ga,Mn)(Bi,As) dilute magnetic semiconductor. *Materials.* 2020. **13**. P. 5507. https://doi.org/10.3390/ma13235507.
11. Yastrubchak O., Riney L., Powers W. *et al*. Band engineering of magnetic (Ga,Mn)As semiconduc-

tors by phosphorus doping. *IEEE Trans. Magn*. 2023. **59**. P. 1600106. https://doi.org/10.1109/TMAG.2023.3287730.
12. Chapman R.A., Hutchinson W.G. Photoexcitation and photoionization of neutral manganese acceptors in gallium arsenide. *Phys. Rev. Lett.* 1967. **18**. P. 822. https://doi.org/10.1103/PhysRevLett.18.443.
13. Scarpulla M.A., Cardozo B.L., Farshchi R. *et al*. Ferromagnetism in $Ga_{1-x}Mn_xP$: Evidence for inter-Mn exchange mediated by localized holes within a detached impurity band. *Phys. Rev. Lett.* 2005. **95**. P. 207204. https://doi.org/10.1103/PhysRevLett.95.207204.
14. Gluba L., Yastrubchak O., Sek G. *et al*. On the nature of the Mn-related states in the band structure of (Ga,Mn)As alloys via probing the E_1 and $E_1+\Delta_1$ optical transitions. *Appl. Phys*. *Lett.* 2014. **105**. P. 032408. https://doi.org/10.1063/1.4891329.
15. Dmitruk N.L., Borkovskaya O.Yu., Mamontova I.B. *et al*. Ultraviolet responsivity control in Schottky barrier heterostructures with textured interface. *Thin Solid Films*. 2000. **364**. P. 280–283. https://doi.org/10.1016/S0040-6090(99)00945-1.
16. Yastrubchak O., Bak-Misiuk J., Łusakowska E. *et al*. Strain release in $InGaAs/In_xAl_{1-x}As/InP$ heterostructures. *Phys. B: Condens. Matter*. 2003. **340–342**. P. 1082–1085. https://doi.org/10.1016/j.physb.2003.09.183.
17. Yastrubchak O., Domagała J.Z., Wosiński T. *et al*. Anisotropic strain relaxation in lattice-mismatched III–V epitaxial layers. *phys. status solidi (c)*. 2005. **2**. P. 1943–1947. https://doi.org/10.1002/pssc.200460530.
18. Fujii J., Salles B.R., Sperl M. *et al.* Identifying the electronic character and role of the Mn states in the valence band of (Ga,Mn)As. *Phys. Rev. Lett.* 2013. **111**. P. 097201. https://doi.org/10.1103/PhysRevLett.111.097201.
19. Donmez O., Gunes M., Henini M., Erol A. Determination of electronic band structure of quaternary ferromagnetic $Ga_{0.97-y}Mn_{0.03}Cr_yAs$ epitaxial layers. *Phys. B: Condens. Matter.* 2023. **665**. P. 415074. https://doi.org/10.1016/j.physb.2023.415074.
20. Mahadevan P., Zunger A. First-principles investigation of the assumptions underlying model-Hamiltonian approaches to ferromagnetism of 3d impurities in III-V semiconductors. *Phys. Rev. B*. 2004. **69**. P. 115211. https://doi.org/10.1103/PhysRevB.69.115211.

Authors and CV

Oksana B. Yastrubchak, PhD in Physics and Mathematics, author of over 60 publications with more than 500 citations and an h-index of 14. Her research focuses on investigating the fundamental properties of magnetic and topological materials through advanced spectroscopic characterization. https://orcid.org/0000-0001-6641-5768

S.V. Mamykin, PhD in Physics and Mathematics, Head of the Department of Kinetic Phenomena and Polaritonics at the V. Lashkaryov Institute of Semiconductor Physics. Author of over 90 publications and 5 patents. The area of scientific interests includes optics, optoelectronics, plasmonics, nanophotonics, sensorics and photoconverting devices.
E-mail: mamykin@isp.kiev.ua,
https:// orcid.org/0000-0002-9427-324X

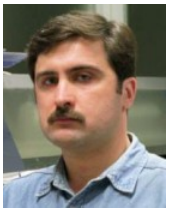

V.R. Romanyuk, PhD in Physics and Mathematics, Senior Researcher at the Department of Kinetic Phenomena and Polaritonics, V. Lashkaryov Institute of Semiconductor Physics. Authored more than 50 articles. The area of scientific interests includes optical materials science and optical diagnostics. E-mail: romanyuk@isp.kiev.ua,
https://orcid.org/0000-0002-0068-5973

Olga S. Kondratenko, PhD in Physics and Mathematics, Senior researcher at the Department of Diagnostics of semiconductor materials, structures and devices, Laboratory of spectral ellipsometry, V. Lashkaryov Institute of Semiconductor Physics. The area of scientific interests includes optoelectronics, plasmonics, optics, nanophotonics, thin films.
E-mail: kondratenko@isp.kiev.ua,
https://orcid.org/0000-0003-1948-4431

Lyudmyla V. Borkovska. Doctor of Sciences in Physics and Mathematics, Head of the Department of Sensor Systems, V. Lashkaryov Institute of Semiconductor Physics. Author of more than 95 articles, 2 patents, and co-author of 7 collective monographs. Field of research: optical sensors, solid-state luminescent materials, light-emitting devices and structures. E-mail: l_borkovska@ukr.net,
https://orcid.org/0000-0002-7832-3796

Larysa Yu. Khomenkova, Doctor of Sciences in Physics and Mathematics, Leading Scientist at the Department of Sensor Systems, V. Lashkaryov Institute of Semiconductor Physics. Author of over 180 scientific publications. The main activity concerns elaboration of multifunctional composite materials for photonics application, catalysis, and alternative energy sources.
E-mail: khomen@ukr.net,
https://orcid.org/0000-0002-5267-5945

Vladyslav V. Kaliuzhnyi, PhD, Junior Researcher at the Department Kinetic Phenomena and Polaronics, V. Lashkaryov Institute of Semiconductor Physics. Author of 8 publications. Expertise: physics of semiconductor materials and devices (HEMTs and HEMT-like structures, III-nitrides), modeling of transport properties. E-mail: vladkaliuzh@gmail.com, https://orcid.org/0000-0003-2084-6938

O.V. Shtykalo, PhD Student, Engineer and IoT Device Developer, V. Lashkaryov Institute of Semiconductor Physics. Expertise: developing and characterization of photovoltaic converters, plasmon-polariton photodetectors and optoelectronic systems based on them.
E-mail: astrosasha013@gmail.com, https://orcid.org/0000-0002-1595-4427

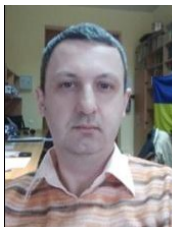

Oleksandr F. Kolomys, PhD in Physics and Mathematics, Senior Researcher at the Laboratory of Submicron Optical Spectroscopy, V. Lashkaryov Institute of Semiconductor Physics. Authored over 130 scientific publications, 3 patents, and 3 textbook chapters. The area of scientific interests includes Raman and luminescent microanalysis of light emitting properties, structure, composition, electronic and phonon excitations in solids.
E-mail: olkolomys@gmail.com, https://orcid.org/0000-0002-1902-4075

Authors' contributions

Yastrubchak O.B.: conceptualization, investigation, formal analysis, visualization, funding, writing – original draft, review & editing.
Mamykin S.V.: conceptualization, methodology, measurements, data analysis, writing – review & editing.
Romanyuk V.R.: investigation, visualization, data analysis.
Kondratenko O.S.: investigation, data analysis, visualization.
Khomenkova L.Yu.: investigation, validation.
Borkovska L.V.: measurements, writing – review & editing.
Kaliuzhnyi V.V.: data analysis.
Shtykalo O.V.: software, device development.
Kolomys O.F.: investigation, formal analysis, validation.
Furdyna J.K.: conceptualization, methodology, discussions.
Liu X.: conceptualization, samples growth, investigation, visualization, discussions.
Assaf B.A.: conceptualization, funding, discussions, writing – original draft.

Ідентифікація ступеня гібридизації Mn-похідних станів у (Ga,Mn)(As,P) засобами спектроскопічної еліпсометрії

О.Б. Яструбчак, С.В. Мамикін, В.Р. Романюк, О.С. Кондратенко, Л.В. Борковська, Л.Ю. Хоменкова, В.В. Калюжний, О.В. Штикало, О.Ф. Коломис, X. Liu, J.K. Furdyna, B.A. Assaf

Анотація. Продемонстровано можливість безпосереднього спектроскопічного контролю Mn-пов'язаних електронних станів у розведеному феромагнітному напівпровіднику (Ga,Mn)(As,P) шляхом вбудовування фосфору в кристалічну ґратку матриці зі сталою концентрацією Mn. За допомогою спектроскопічної еліпсометрії ми спостерігаємо послідовний перехід від *p–d* гібридизованих станів Mn за низького вмісту P до локалізованих, атомоподібних *d*-станів Mn за високої концентрації P. Ця еволюція проявляється у вигляді переходу від широких смуг оптичного поглинання (2.0–2.8 еВ), які послаблюються під час відпалу, до вузького, нечутливого до відпалу, піка поглинання (2.6–2.9 еВ), що супроводжується залежним від вмісту P зсувом валентної зони відносно рівня Фермі. Отримані результати підтверджують, що заміщення фосфором можна використати як незалежний параметр керування електронною гібридизацією між домішковими станами Mn та валентною зоною матриці. Суттєва зміна характеру спектральних особливостей, пов'язаних із Mn, свідчить про те, що легування фосфором змінює баланс між делокалізованими (валентнозоноподібними) та локалізованими Mn-похідними станами. Наші дослідження показують, що природа Mn-пов'язаних станів безпосередньо визначається складом матеріалу.

Ключові слова: розбавлені феромагнітні напівпровідники, *p–d* гібридизація, сплави (Ga,Mn)(As,P), спектроскопічна еліпсометрія.